NACA TN 3488

NATIONAL ADVISORY COMMITTEE FOR AERONAUTICS

TECHNICAL NOTE 3488

SOME MEASUREMENTS OF FLOW IN A RECTANGULAR CUTOUT

By Anatol Roshko

California Institute of Technology

Washington
August 1955

NATIONAL ADVISORY COMMITTEE FOR AERONAUTICS

TECHNICAL NOTE 3488

SOME MEASUREMENTS OF FLOW IN A RECTANGULAR CUTOUT

By Anatol Roshko

SUMMARY

The flow in a rectangular cavity, or slot, in the floor of a wind tunnel is described by the results of pressure and velocity measurements. Pressure distributions on the cavity walls as well as measurements of friction are presented. The effects of varying depth-breadth ratio are shown.

INTRODUCTION

This report is an account of some measurements of the pressure and velocity fields set up by the flow over a rectangular cavity, or groove, in the floor of a wind tunnel. There exists at present little quantitative information about the flow in this or other cutouts in aerodynamic surfaces. In the visualization techniques that have been employed, the principal result is to show the existence of a vortex, or system of vortices, within the cavity. The equilibrium of such vortex systems must evidently depend on the geometry of the cavity and the parameters of the outside flow, for example, boundary-layer thickness. However, it is not at all apparent which features are predominant in determining this equilibrium, and there appear to be no published measurements which might help in setting up a model.

Some quantitative results are given in two papers by Wieghardt (ref. 1) and Tillmann (ref. 2), where a few other references will also be found. Their results for cavities are part of a larger study of the drag of surface irregularities. In addition to some aluminum-powder pictures in reference 1, their results for cutouts consist principally of the drag coefficients, obtained by subtracting the drag values of the aerodynamic surface with and without cutout. It was also found that a systematic variation of the depth-breadth ratio of a given cavity gave a "periodic" variation of the cavity drag coefficient, showing definite peaks. The net cavity drag must include the effects of pressure on the cavity walls, the friction on the floor, and the change of friction which is effected on the aerodynamic surface by the presence of the cavity. Without further study of these components it is difficult to explain the drag variations and, more fundamentally, to get some understanding of the flow mechanism.

In addition to the interest in the effects on drag, there is another practical problem arising from the fluctuating pressures and velocities which may exist in and near a cavity. Fairly violent fluctuations are often observed; they may be due either to the turbulence of the flow or to intermittencies connected with instabilities of the vortex system. Such problems in aeronautics arise, for instance, in connection with bomb bays, open cockpits, escape hatches, and so forth. There also exist, of course, many nonaeronautical examples.

Probably of even more interest from the fundamental point of view is the problem of the vortex mechanism itself. It appears that in most of the flow problems involving separation, for instance, the base-pressure problem, the flow past bluff bodies, and even diffuser separation, the formation of reverse flows and vortices is an important part of the mechanism. In most cases the vortices are nonsteady, making an experimental study rather difficult. In a cavity, on the other hand, there is the possibility of obtaining a stationary, captive vortex and of gaining from it some understanding of the mechanics of real vortices.

Finally, there is the phenomenon of sound production in high-speed flow past such cavities, reported in reference 3. The production of these regular, periodic, high-intensity sound waves is not understood. One possibility is that they are associated with movements of the vortices in the cavity, the frequency being determined by the coupling between the acoustic field and the vortex field. The cavities used in the study of reference 3 were too small to permit a detailed investigation of the flow inside them. It was intended that the present study, made on a much larger cavity, should provide some information that might be useful in the acoustic problem.

The work, which was conducted under the sponsorship and with the financial assistance of the National Advisory Committee for Aeronautics, is part of a program of turbulence and aerodynamic-noise studies at the Guggenheim Aeronautical Laboratory, California Institute of Technology. The author received valuable assistance from Mrs. Dietlind Wegener and Mr. Johannes de Bruyn, who helped with the measurements and reduction of data.

SYMBOLS

b	breadth of cavity
C_D	drag coefficient of cavity, based on breadth
C_F	friction coefficient

C_p	pressure coefficient
d	depth of cavity
p	static pressure
p'	pitot pressure
p_1	static pressure at reference point
U_∞	free-stream velocity
u	magnitude of velocity anywhere in flow
x	distance measured along flow direction
y	distance measured normal to any surface
μ	coefficient of viscosity
ρ	density

EXPERIMENTAL ARRANGEMENT

The measurements were made in the Merrill Wind Tunnel at the California Institute of Technology. This has a vented test section 42 inches wide and 36 inches high and may be operated at speeds up to 160 mph.

The cavity consisted of an open, Duralumin box set into the tunnel floor as shown in figure 1. The box opening was of fixed dimensions, 4 inches by 32 inches, with the long side normal to the flow.

The depth of the cavity could be varied from 0 to 10 inches by changing the position of the bottom. This could be set at any depth by means of the screw jack to which it was attached. The corners between the bottom and the sides were not sealed during the measurements. A comparison of pressure distributions with and without sealing indicated negligible difference; thus considerable inconvenience was avoided by not having to seal after each change of depth.

It will be noted that the box flanges, resting on the tunnel floor, were not set flush. Since it was necessary, in any case, to use whatever boundary layer already existed on the tunnel floor, the 3/16-inch flange made no essential difference to the goal of the experiments.

The sides, bottom, and flanges of the box were equipped with static holes for static-pressure measurements. In addition, there were access holes for admitting pitot probes. Of standard type with flattened openings, each pitot tube could be traversed normal to the surface by means of a micrometer head mounted outside the box. The locations of the static holes and pitot tubes are indicated by sketches in the figures in which the results are presented.

RESULTS

In the results of the measurements, which appear in figures 2 to 9, distances have been normalized by the streamwise breadth of the cavity b, which had the fixed value of 4 inches. Most of the runs were made at a nominal tunnel speed of 75 feet per second; some additional measurements were made, for comparison, at 210 feet per second.

The free-stream velocity U_∞ was actually measured at a static orifice $1\frac{1}{2}$ inches upstream of the cavity, the pitot pressure being measured outside the tunnel boundary layer. This velocity was used to normalize the measured pressures, which were always measured relative to the pressure p_1 at an orifice 1/2 inch ahead of the cavity:

$$C_p = \frac{p - p_1}{\frac{1}{2}\rho U_\infty^2}$$

Skin-friction coefficients were obtained from velocity profiles using the relation

$$C_F = \frac{\mu}{\frac{1}{2}\rho U_\infty^2}\left(\frac{du}{dy}\right)_{wall}$$

Static Pressures on Cavity Bottom

Figure 2 shows the pressure distributions on the bottom for several different depths. The results here are mainly for shallow cavities of depth-breadth ratios $d/b = 0.016$, 0.031, 0.047, 0.063, and 0.094. In addition, the results for deeper cavities with $d/b = 0.25$ and $d/b = 1$ are shown for comparison.

In all cases but the shallowest there is initially a drop in pressure downstream of the front edge, followed by a rather rapid rise. (Even in the shallowest case there may be a similar behavior; the orifice spacing was not close enough to resolve this.) This initial behavior is typical of the base-pressure problem, that is, flow over a step. Over most of the remainder of the bottom, the pressure increases at first with increasing depth, but eventually it begins to decrease. There is a kind of upper envelope to the set of curves at pressure coefficients of the order of 0.2. It will be observed that the pressures in the shallow cavities are considerably higher than those in the deeper ones of $d/b = 0.25$ and 1.

The outer portions of the curves are shown dotted, for it was not possible to obtain measurements out to the bottom corners. Instead, the curves are faired into the points measured at the top back corner and at orifice 1, 1/2 inch ahead of the cavity.

The variation of pressure with depth is shown more explicitly in figure 3. For this, the pressure at a single point, orifice 14, at the center of the bottom was chosen for study. Figure 3 shows how the pressure coefficient there first rises and then falls as the bottom is lowered, attaining a maximum value of about 0.18 at $d/b = 0.06$. Essentially the same result is obtained for both speeds, 75 and 210 feet per second. Included in the same figure are measurements of the pitot pressure p' obtained with a flattened pitot tube set close to the bottom surface at station 14 and facing upstream. These measurements indicate that separation occurs at station 14 soon after the maximum pressure is reached.

The relation of the shallow-cavity regime to deeper cavities is shown in figure 4 where the static pressure at station 14 was measured for depths up to 10 inches. The C_p values of figure 3 are included on a rather more compressed scale. The shallow-cavity regime stands out clearly in relation to the whole range. The extended points shown by bars indicate pressures which varied intermittently. The intermittent regions occur at values of d/b from about 0.5 to 0.87 and above 2. The change from intermittent to steady pressures at $d/b = 0.87$ occurs quite sharply. Some tuft studies indicated that a steady, single vortex in the cavity is first formed at this value of the depth.

Pressure at Downstream Top Corner

The pressure distributions for the shallow cavities show a steep pressure rise at the downstream end. Apparently the boundary layer, which separates at the front edge, diffuses into the cavity, so that the velocity on the streamline approaching the downstream edge has some value greater than zero. This value increases, at first, as the depth

is increased, and consequently the stagnation pressures near the back edge increase at first. When the cavity depth exceeds a certain value ($d/b \approx 0.1$), the separated boundary layer no longer reattaches to the bottom. It is probably at about this value that a general vortex system is first set up, in contrast with shear-layer diffusion at shallower depths.

With the expectation that the pressure near the back edge should be sensitive to changes of flow regime, measurements were made there by means of a small pitot tube set on the top surface, as shown in the sketch of figure 5, at the position marked 30. The center of the pitot orifice was actually about 0.01 inch above the edge, but it may be expected to give a fair measure of the pressure on the cavity wall immediately below the edge, except for the shallowest cavities. The variation of the pressure at station 30 with varying depth is shown in figure 5. Because of the finite height of the orifice above the edge, the values at very shallow depths are in error; at $d = 0$ the value of C_p should actually be zero. As d decreases, the expected pressure peak is obtained, followed by a minimum, at about $d/b = 0.2$. The range of intermittent changes observed previously again appears, while at larger depths there is a hysteresis loop. In the vicinity of $d/b = 1$ the absence of hysteresis and intermittency indicates the stability of the single vortex in a cavity of square section.

The pressure at station 30 remains at a relatively high level for all depths.

Pressure Distributions on Cavity Walls

For the larger depths, pressure distributions were obtained on the cavity walls as well as on the bottom. These are given in figures 6(a) to 6(f).

Figure 6(b), against which the others may be conveniently compared, shows the distribution in a cavity of square section $d/b = 1$. The pressures at all points were steady. (To understand the plotting of the figure, it is to be noted that the values for the walls are plotted on the same abscissa as those for the bottom; that is, the curves show the continuous variation of pressure along the perimeter.) The lower pressures near the center of the walls and bottom and the high pressures at the corners are typical of the single, stable vortex. The contribution to the cavity drag of the pressure on the walls gives $C_D = 0.033$.

The value at station 30 is off scale, but it will be noted that there is a rather abrupt transition to much lower pressures on the top surface downstream of the edge.

The figure includes measurements taken with and without sealing of the bottom corners. (Tape was used for sealing.) It shows the negligible effect of leaving the corners unsealed.

Also shown is the distribution for U_∞ = 210 feet per second, for comparison with the case of U_∞ = 75 feet per second. There is no essential difference, but the higher value of U_∞ gives somewhat larger amplitudes of pressure coefficient, which may be taken as indication of a "stronger" vortex.

Figure 6(a) shows the results of similar measurements for a gap of $d/b = 0.75$, that is, a value slightly below that at which a single, stable vortex first forms. The intermittent nature of the flow is indicated by the variations of pressure, which are represented by the bars. These correspond to the excursions of pressure observed on the alcohol manometer. They are not periodic vibrations but rather erratic, intermittent variations. No account was taken of the damping and inertia of the alcohol manometer, so that the recorded changes are not necessarily the exact pressure variations in the cavity. They are presented primarily for comparison with the results for the cavity of square section.

Additional measurements of pressure distribution in cavities having d/b ratios of 0.875, 1.5, 2, and 2.5 are shown in figures 6(c) to 6(f), plotted on a smaller scale. The value $d/b = 0.875$ is just above that at which a single, stable vortex first forms. It is similar to the case of $d/b = 1$ but gives a slightly stronger vortex in terms of the pressure amplitudes obtained.

At $d/b = 1.5$ the pressure distributions on the wall indicate a stationary vortex in the upper part of the cavity. The pressure distribution on the floor, however, is not like that due to a single vortex. It appears that there is a small-scale vortex structure in the lower part of the cavity, with a single, main vortex in the upper part.

Similar remarks apply to the larger values of d/b. In addition, the main vortex appears to become weaker with increasing values of d/b.

The most important point to note in these figures is the steep pressure rise near the top downstream edge, in all cases. This, as explained above, is evidently due to the pressure built up near that corner as part of the separated boundary layer is deflected into the cavity.

Boundary Layer on Wind-Tunnel Floor

Figure 7 shows the velocity profiles measured in the boundary layer on the tunnel floor at several stations upstream and downstream of the cavity. The one at station 2, at $1\frac{1}{2}$ inches upstream, is representative of the flow ahead of the cavity. It is little affected by the depth.

For station 27, at $1\frac{1}{2}$ inches downstream, two measurements are shown, one for the cavity of square section and one for the case of no cavity, that is, bottom flush with the surface. These two cases give a measure of the effect of the cavity on the skin friction of the primary surface. The change of skin friction, calculated from the velocity profiles, was from 0.0014 to 0.0012.

Measurement at station 26, at 1/2 inch downstream of the cavity, shows an even greater decrease of friction there. Thus, the effect of the cavity, at least of the one of square section, is to decrease the skin friction on the main surface. It appears then that the net drag increment which is observed for such cavities (of order 0.02, according to ref. 2) must be accounted for by the pressures on the walls. (Any friction on the bottom will contribute a thrust, in the cavity of square section.)

Friction on Cavity Walls

The cavity of square section was selected for a few measurements of skin friction on the cavity walls. Figure 8 shows the profiles obtained. The left-hand side of the figure is for U_∞ = 210 feet per second, while the right-hand side is for U_∞ = 75 feet per second. In each case the profiles were measured at three points - the centers of the downstream wall, bottom, and upstream wall, which are stations 23, 14, and 5, respectively. From the results of the pressure distributions it is expected that maximum values of shear will be obtained at those points. (Possibly they will be higher on the upper part of the downstream wall.) The skin-friction coefficients, which were computed from the slopes of the velocity profiles, extrapolated to 0, have the following values: For 210 feet per second at stations 23, 14, and 5, C_F = 0.00044, 0.00038, and 0.00041, respectively; while for 75 feet per second they are 0.00074, 0.00066, and 0.00054. More extensive investigations of friction distributions were not made; the important result is that the friction coefficients are two orders of magnitude lower than the pressure coefficients and the pressure-drag coefficient.

Velocity Profile in Captive Vortex

The velocity profiles shown in figure 8 include only the region immediately next to the wall. They were easily extended to greater distances by simply traversing the pitot probe further into the cavity. However, since the static pressure was still measured on the wall, it was felt that the measurements could not be extended to more than about 0.2 inch from the wall without requiring the use of a pitot static probe. At greater distances from the wall the measurements are also made more

difficult by the need to aline the probe with the flow direction at each point. Furthermore, near the center of the vortex the mean velocities are low, while the turbulent velocities are comparatively large, so that measurement of velocity there, either by pressure probe or hot-wire, is not straightforward.

Nevertheless, the distance of about 0.2 inch, within which the measurements were considered reliable, is large enough to show that a maximum velocity is reached at a small distance from the wall. The results of measurements at stations 5 and 23, at the centers of the opposite walls, are shown in figure 9. The dotted line joining the two regions of measurement is probably a reasonable estimate of the profile across the center of the cavity. It is roughly that of a vortex in solid-body rotation, with the vortex separated from the walls by thin friction layers. The vortex is, however, not perfectly symmetrical, possibly because of the effects of the friction, so that the velocity maximum on the upstream side is lower than that on the downstream side. These maximum values are $u/U_\infty = 0.27$ and 0.41, respectively. At the center of the floor the measured maximum was 0.30.

CONCLUDING DISCUSSION

Although the measurements made here are by no means complete enough to describe all aspects of the flow in cavities, they do bring out some of the prominent features, as follows:

(1) In a cavity of square section there is a strong tendency to form a single, stable vortex. This is corroborated by the pictures of Wieghardt (ref. 1) and by some exploratory measurements which were made in a 1/2-inch cavity on a surface with laminar boundary layer. The tendency to form a single vortex in a cavity of square section does not seem to depend importantly on the state of the boundary layer ahead of the cavity. However, the pressures and forces due to the flow may be expected to depend on the state of the boundary layer. (Some of Wieghardt's pictures show, in addition to the large, main vortex, small vortices, like "roller bearings," in the corners. These do not invalidate the argument that the mechanism in a square cavity depends essentially on one large vortex; they result from local separation at the corners due to the adverse gradients there.)

(2) The drag increment due to a cavity is almost entirely accounted for by the pressures on the walls. Contrary to what has been supposed, the contribution from the change of friction on the main surface is relatively small.

(3) The friction forces on the cavity walls or, conversely, of the cavity walls on the vortex, are small compared with the pressure forces. Even the friction forces on the free side of the vortex, which can hardly be larger than the skin friction ahead of the cavity, are an order of magnitude smaller than the pressures. This may be useful in setting up a model of the flow; for, if the friction forces on the vortex may be neglected, then the problem should be simplified. Some additional measurements are needed to determine whether the fluid in the cavity may be considered to be isolated or whether there is transport into and out of the cavity. The latter seems the more likely case; for, if the friction forces on the free side are too small to balance the pressure drag, then there must be transport of momentum into the cavity.

(4) The friction forces, though negligible in determining the equilibrium of the vortex, may play a part in determining its stability.

(5) The formation of the vortex occurs by the deflection of part of the separated boundary layer into the cavity, this deflection occurring at the downstream edge and creating a relatively high pressure on the cavity wall in that vicinity. The pressure there accounts for most of the drag. In fact, the variations in drag with varying depth, reported in reference 2, are analogous to the variations of pressure at the downstream edge shown in figure 5. However, it is not likely that the drag can be computed by considering only that point, without taking into account the equilibrium between the vortex and the outer flow. An experiment made to investigate this point consisted of raising the height of the downstream edge 1/4 inch by adding a strip of metal. It was found that the flow in the cavity of square section was not appreciably altered. Apparently, the outer flow, in particular, the separation ahead of the cavity, adjusts itself in such a way that the equilibrium conditions are met by roughly the same kind of vortex inside the cavity.

(6) The stagnation pressures at the downstream edge may be important in the problem of sound production by cavities in high-speed flow. Indeed, schlieren pictures of the phenomenon show that this edge is one source of the sound waves. Any fluctuations of the vortices in the cavity, or of the separated boundary layer, would result in a fluctuation of the stagnation streamline and thereby a variation in the pressure at the back edge.

(7) The intermittencies that are observed to occur, and which may create strong pressure and velocity variations, appear to be due to "switching" back and forth between two possible stable states. They occur for configurations intermediate to those for which stable systems may exist. The intermittency phenomenon is analogous to the large fluctuations of drag which occur on a bluff cylinder in the critical range of Reynolds number.

California Institute of Technology,
Pasadena, Calif., August 6, 1954.

REFERENCES

1. Wieghardt, K.: Erhöhung des turbulenten Reibungswiderstandes durch Oberflächenstörungen. Forschungsbericht 1563, ZWB, Mar. 19, 1942. (Also Jahrb., deutschen Luftfahrtforschung, 1943, pp. 1-17.)

2. Tillmann, W.: Neue Widerstandsmessungen an Oberflächenstörungen in der turbulenten Reibungsschicht. Untersuchungen und Mitteilungen Nr. 6619, ZWB, Dec. 27, 1944. (Available in English translation as NACA TM 1299.)

3. Krishnamurty, K.: Acoustic Radiation From Two-Dimensional Rectangular Cutouts in Aerodynamic Surfaces. NACA TN 3487, 1955.

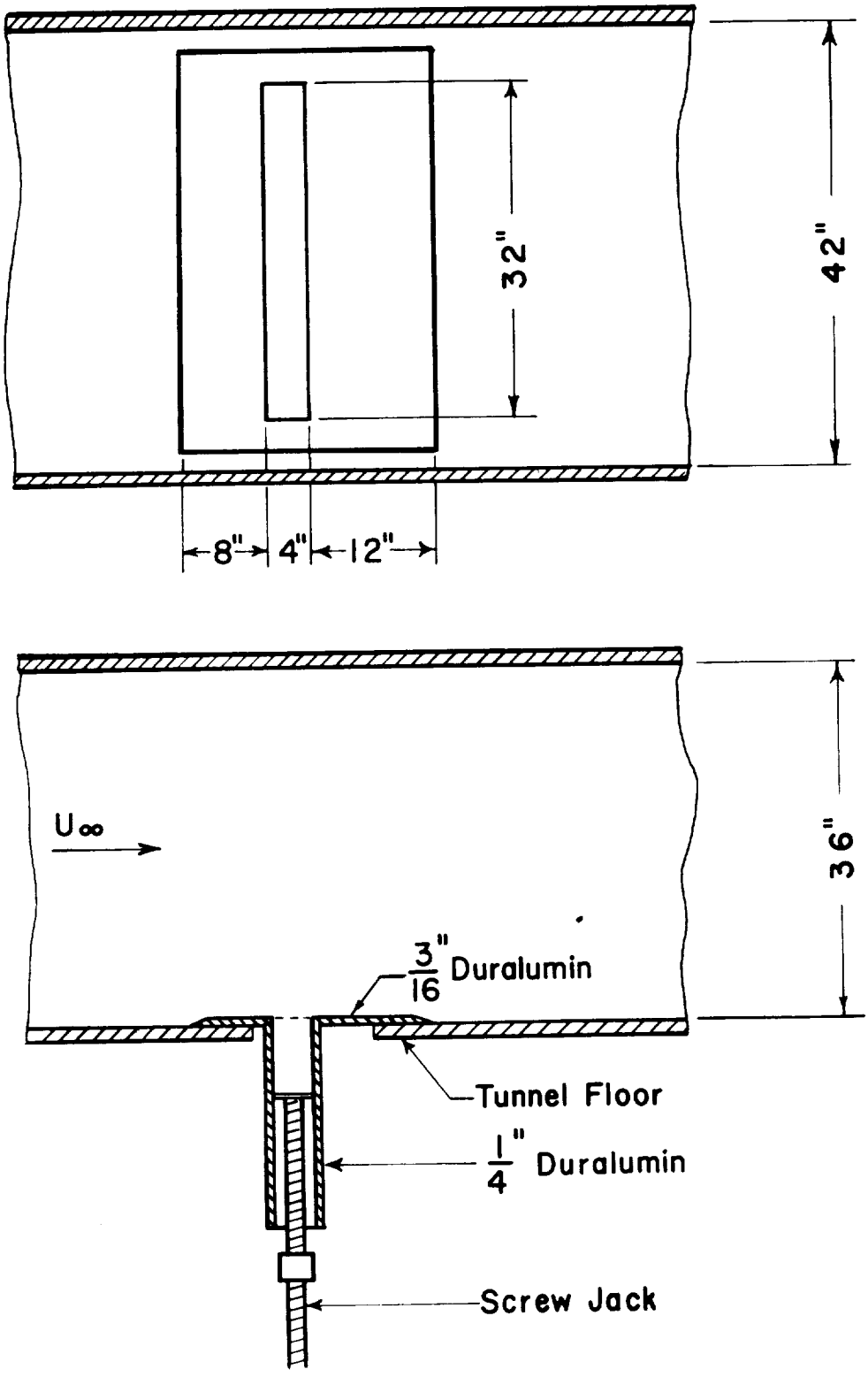

Figure 1.- Arrangement of cavity in test section.

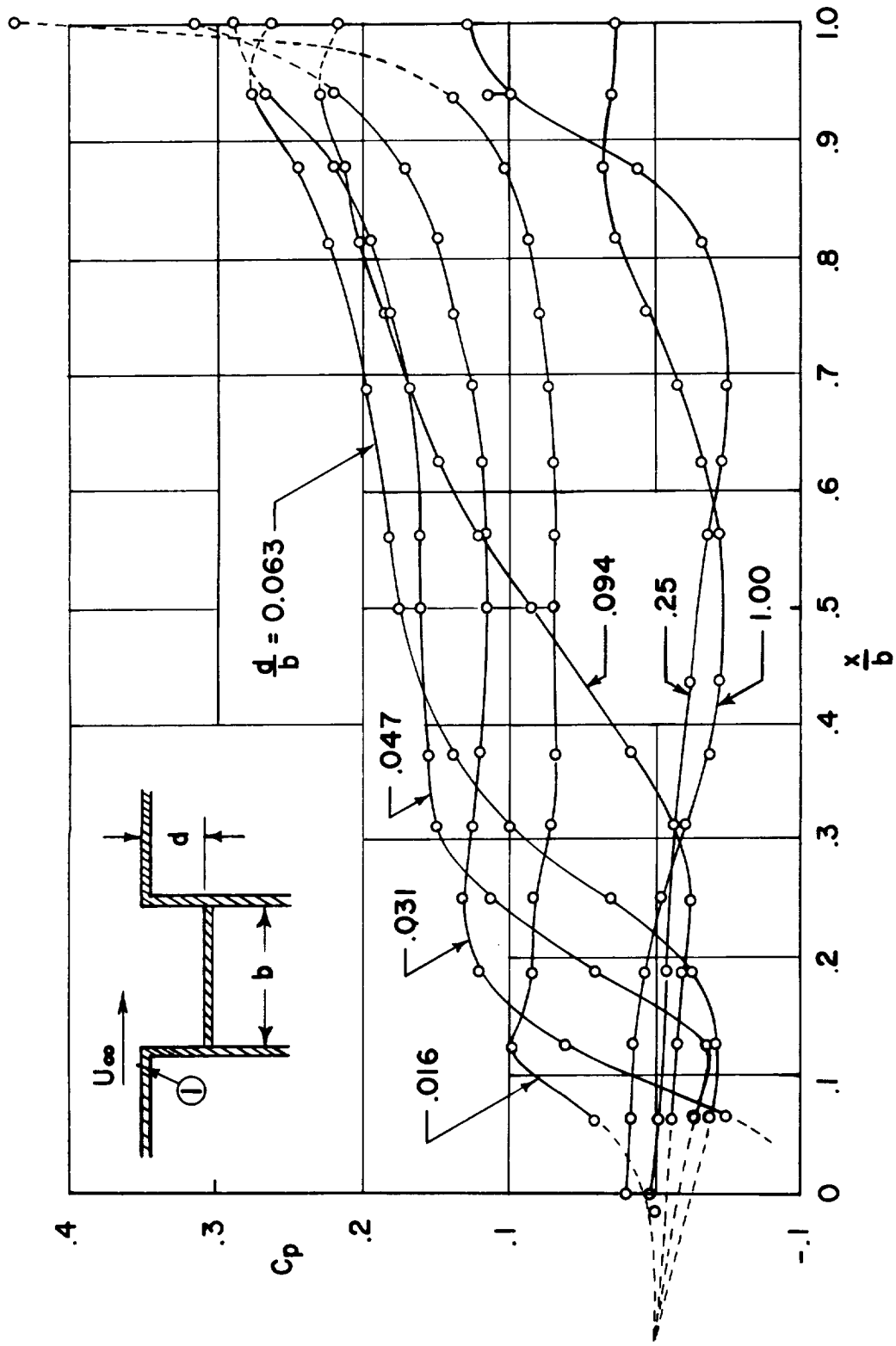

Figure 2.- Pressure distributions on floor. U_∞ = 75 feet per second.

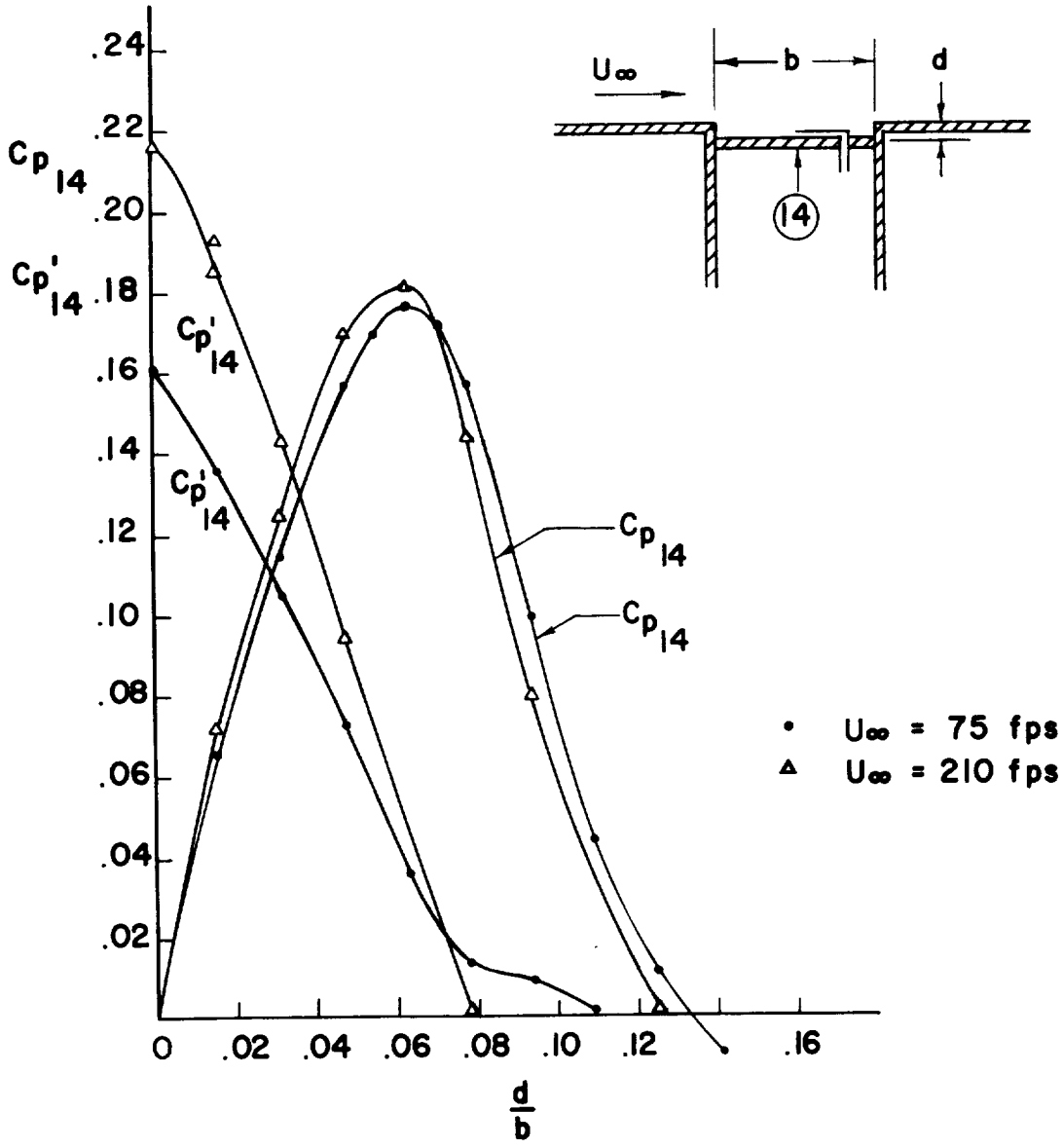

Figure 3.- Effect of depth on pressures at center of floor. (Shallow cavities.)

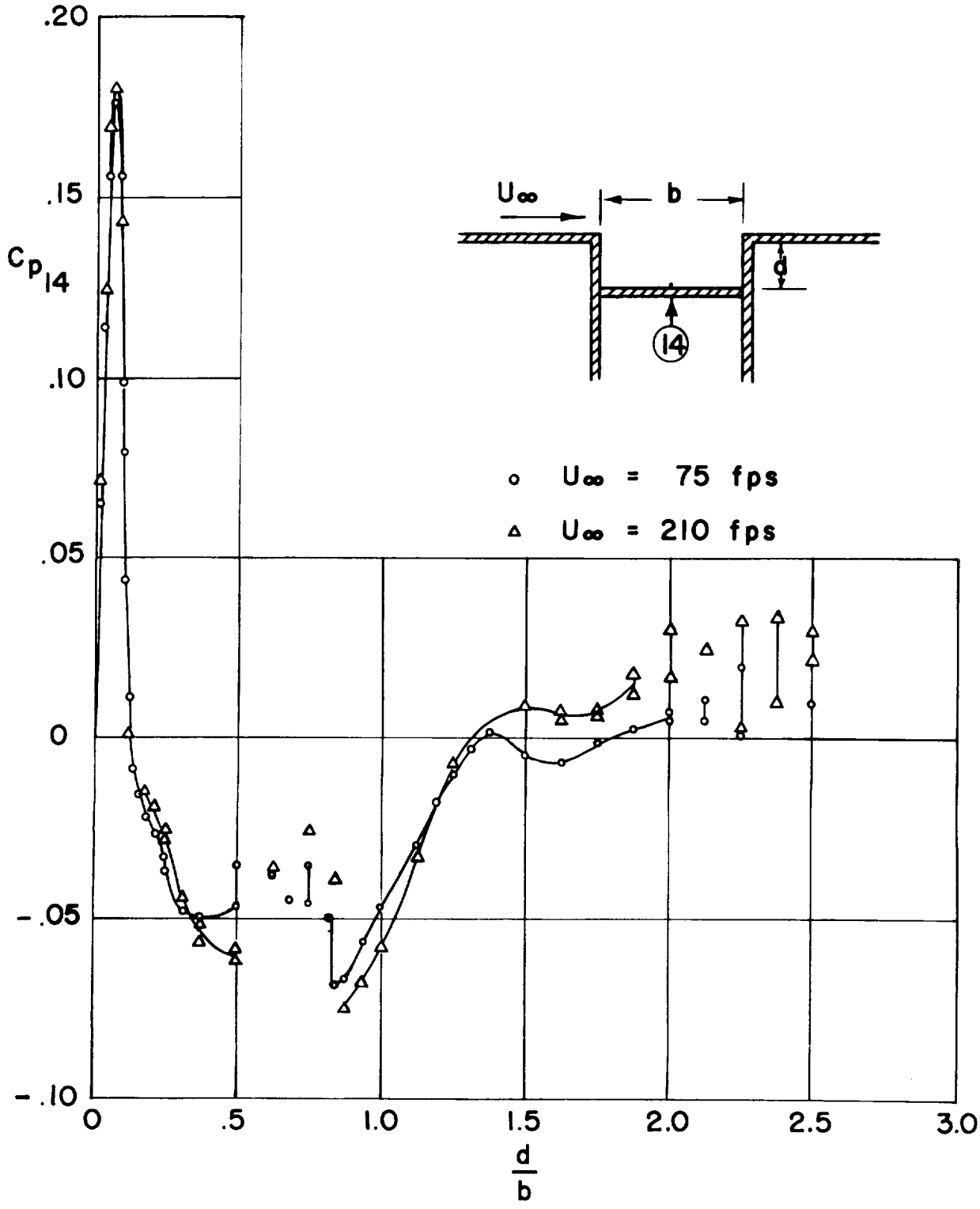

Figure 4.- Relation of shallow-cavity regime to deeper cavities.

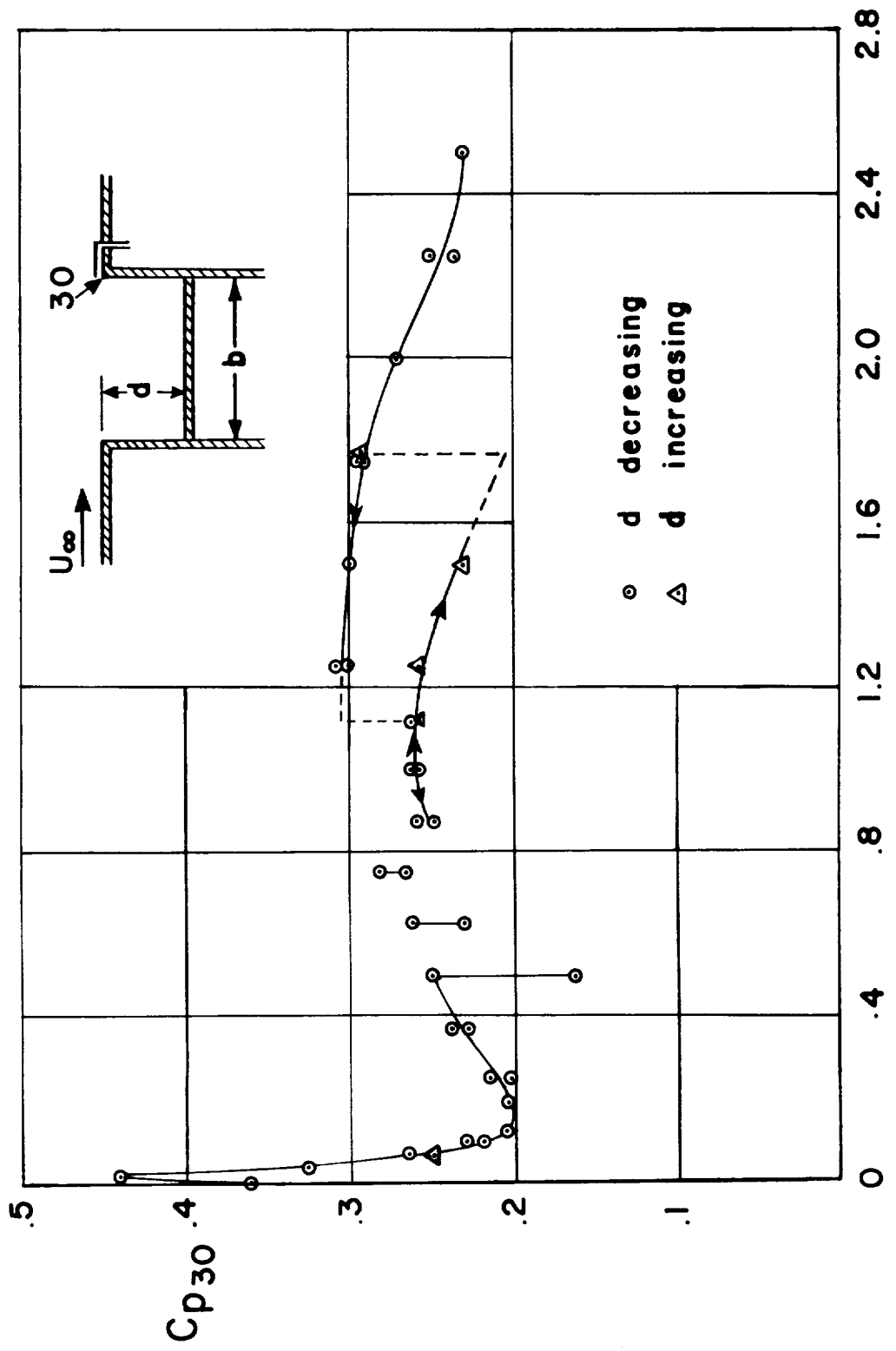

Figure 5.- Pressure at top back corner. U_∞ = 75 feet per second.

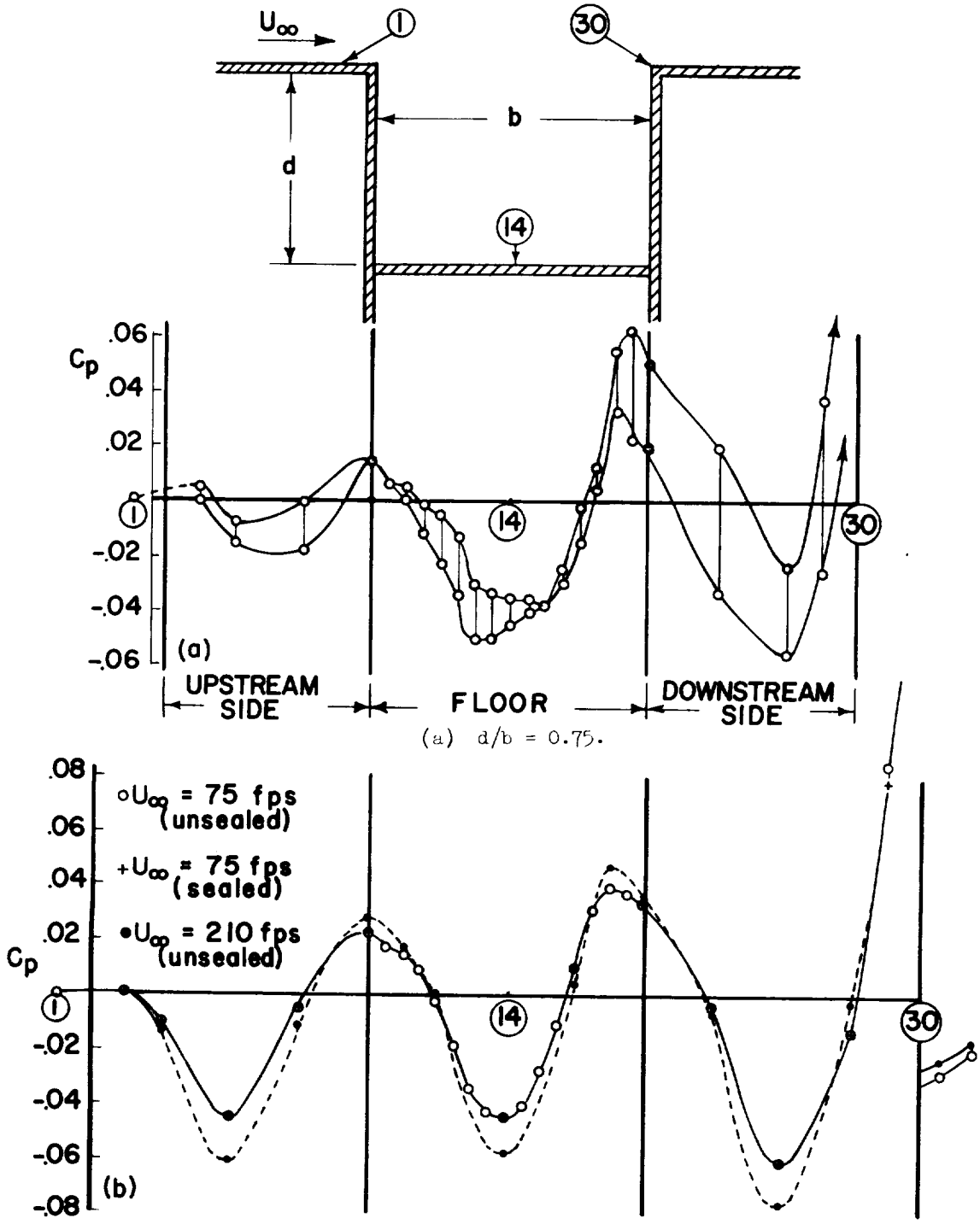

(a) d/b = 0.75.

(b) d/b = 1.00.

Figure 6.- Pressure distribution on cavity walls.

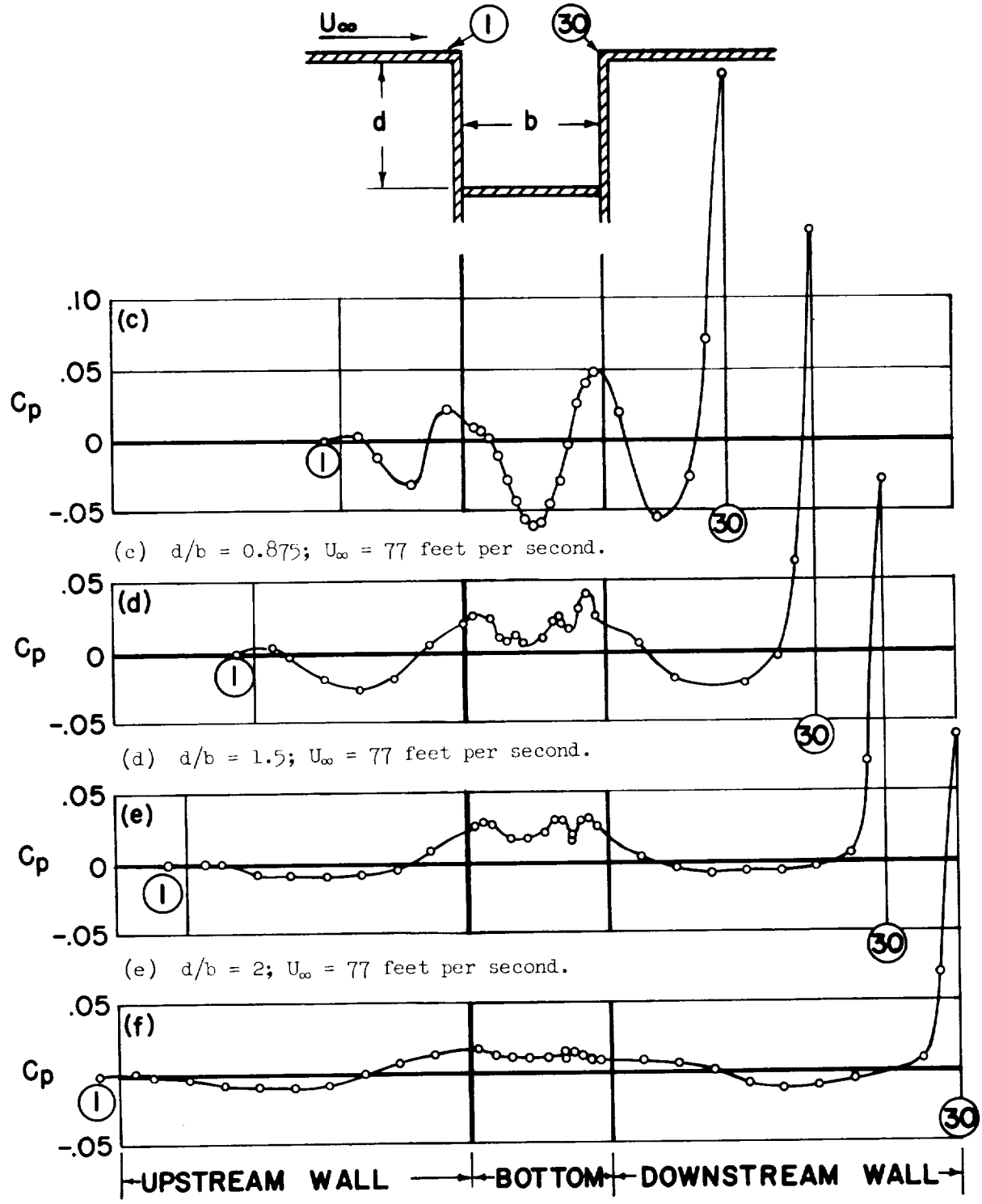

(c) d/b = 0.875; U_∞ = 77 feet per second.

(d) d/b = 1.5; U_∞ = 77 feet per second.

(e) d/b = 2; U_∞ = 77 feet per second.

(f) d/b = 2.5; U_∞ = 77 feet per second.

Figure 6.- Concluded.

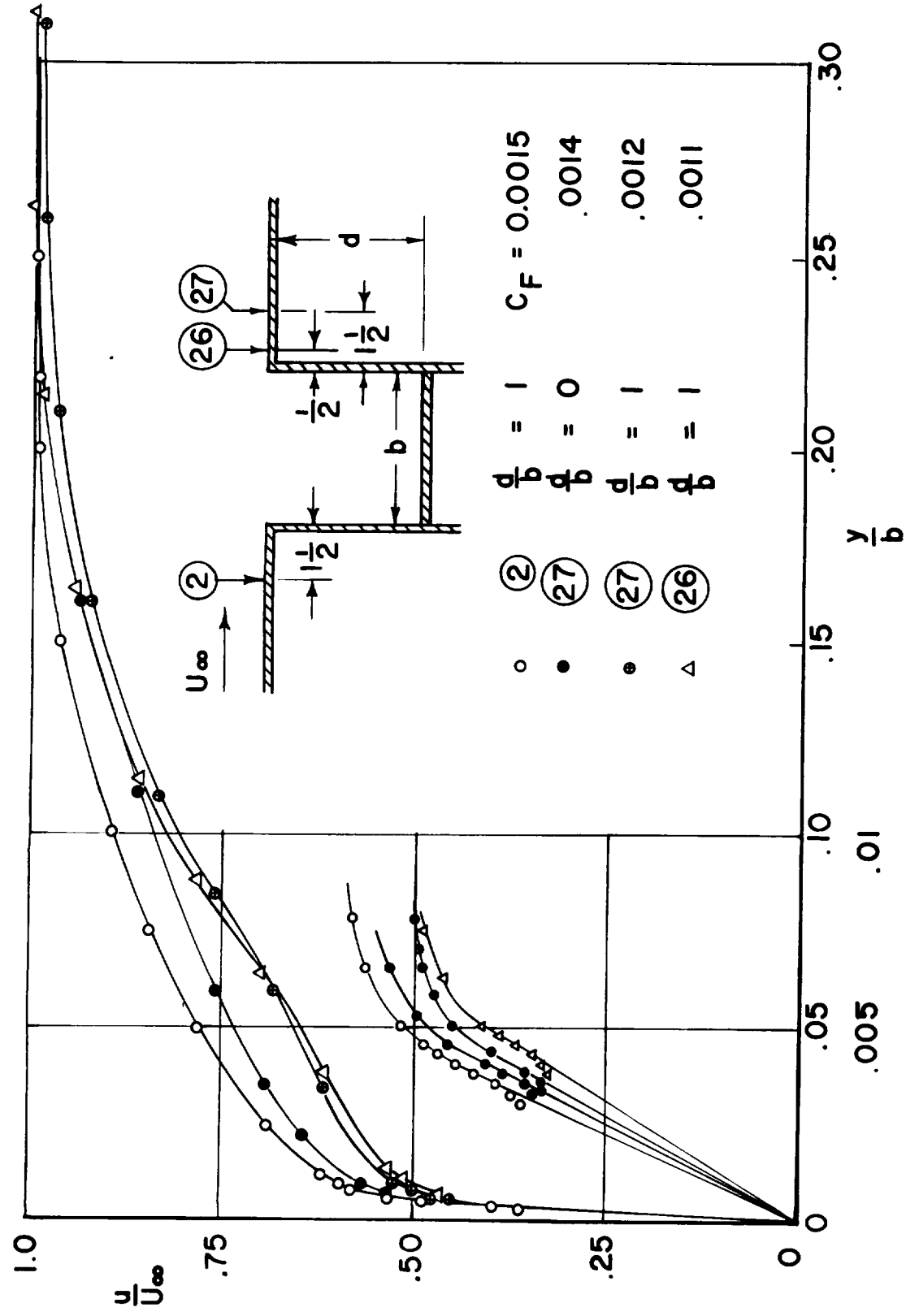

Figure 7.- Boundary layer on test-section wall. U_∞ = 75 feet per second.

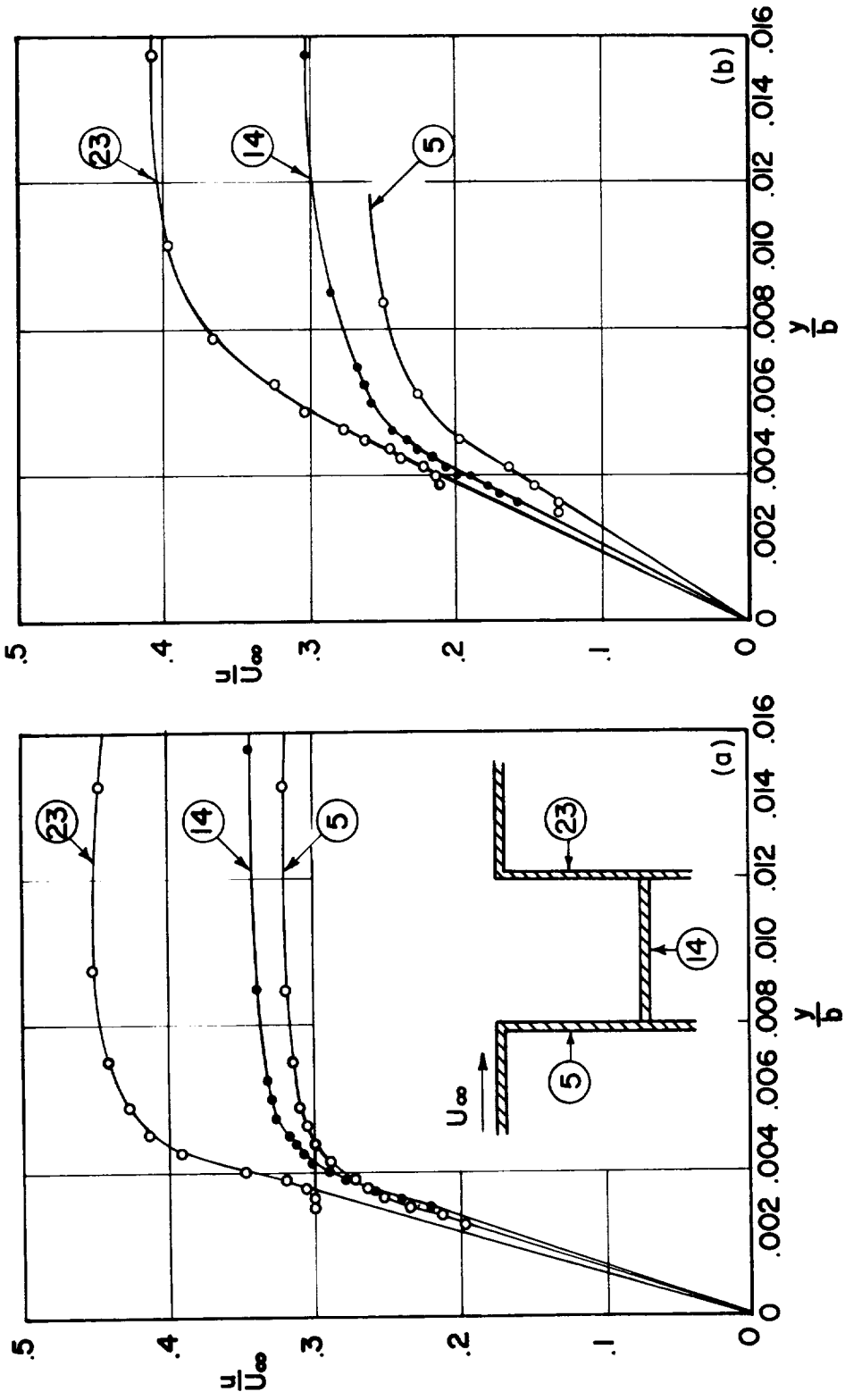

(a) U_∞ = 210 feet per second; $\frac{d}{b} = 1$.

(b) U_∞ = 75 feet per second; $\frac{d}{b} = 1$.

Figure 8.- Velocity profiles on cavity walls.

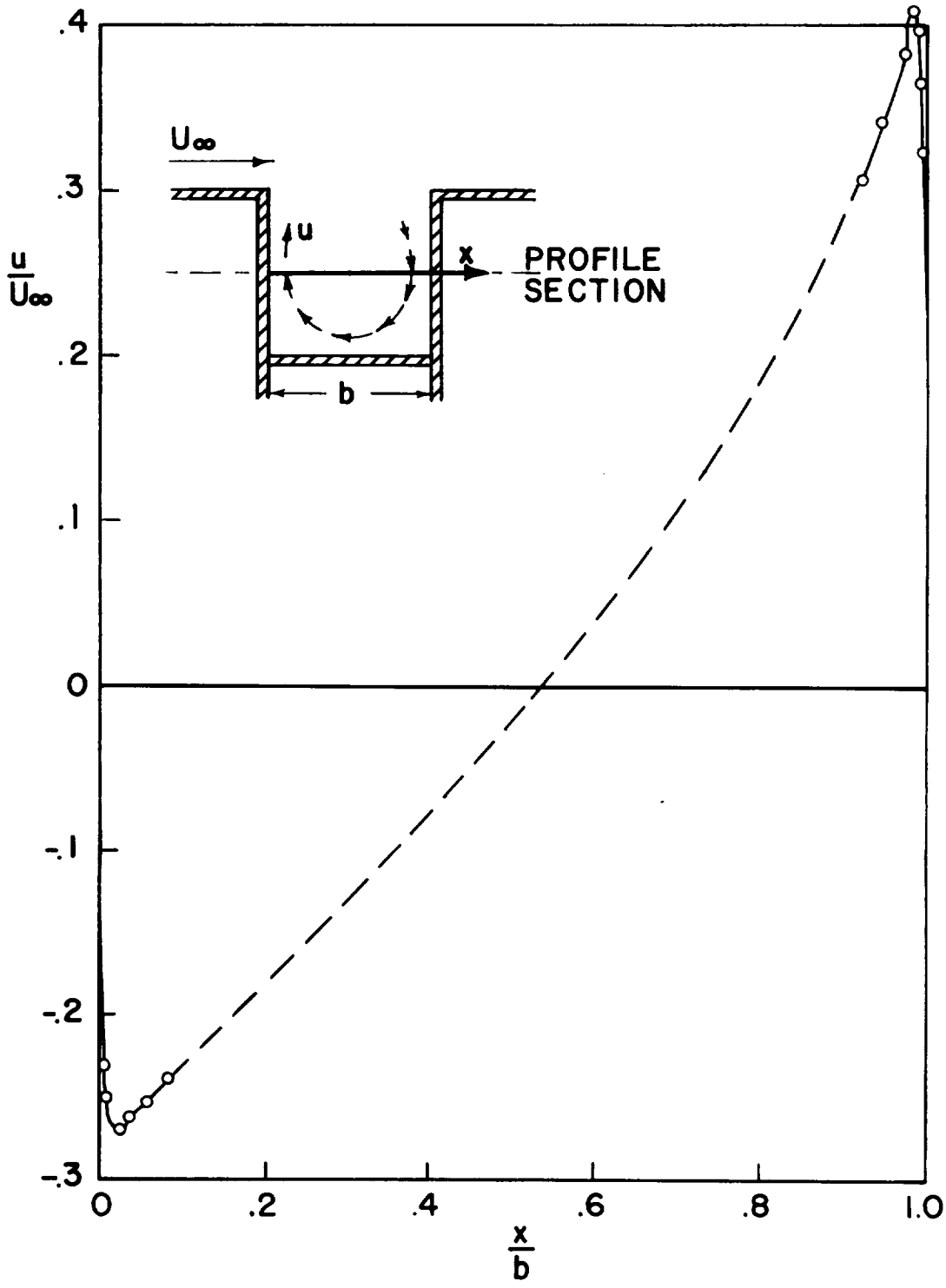

Figure 9.- Estimated velocity profile across cavity. U_∞ = 75 feet per second.